# Hepatocyte nuclear factor-1β regulates Wnt signaling through genome-wide competition with β-catenin/lymphoid enhancer binding factor

Siu Chiu Chan[a], Ying Zhang[b], Marco Pontoglio[c], and Peter Igarashi[a,1]

[a]Department of Medicine, University of Minnesota, Minneapolis, MN 55455; [b]Minnesota Supercomputing Institute, University of Minnesota, Minneapolis, MN 55455; and [c]Department of Development, Reproduction and Cancer, Institut Cochin, Institut National de la Santé et de la Recherche Médicale U1016/Centre National de la Recherche Scientifique Unité Mixte de Recherche 8104, Université Paris-Descartes, Paris, France

Edited by Janet Rossant, Hospital for Sick Children, University of Toronto, Toronto, Canada, and approved October 18, 2019 (received for review June 3, 2019)

**Hepatocyte nuclear factor-1β (HNF-1β) is a tissue-specific transcription factor that is essential for normal kidney development and renal tubular function. Mutations of HNF-1β produce cystic kidney disease, a phenotype associated with deregulation of canonical (β-catenin–dependent) Wnt signaling. Here, we show that ablation of HNF-1β in mIMCD3 renal epithelial cells produces hyperresponsiveness to Wnt ligands and increases expression of Wnt target genes, including *Axin2*, *Ccdc80*, and *Rnf43*. Levels of β-catenin and expression of Wnt target genes are also increased in HNF-1β mutant mouse kidneys. Genome-wide chromatin immunoprecipitation sequencing (ChIP-seq) in wild-type and mutant cells showed that ablation of HNF-1β increases by 6-fold the number of sites on chromatin that are occupied by β-catenin. Remarkably, 50% of the sites that are occupied by β-catenin in HNF-1β mutant cells colocalize with HNF-1β–occupied sites in wild-type cells, indicating widespread reciprocal binding. We found that the Wnt target genes *Ccdc80* and *Rnf43* contain a composite DNA element comprising a β-catenin/lymphoid enhancer binding factor (LEF) site overlapping with an HNF-1β half-site. HNF-1β and β-catenin/LEF compete for binding to this element, and thereby HNF-1β inhibits β-catenin–dependent transcription. Collectively, these studies reveal a mechanism whereby a transcription factor constrains canonical Wnt signaling through direct inhibition of β-catenin/LEF chromatin binding.**

Wnt | transcription | polycystic kidney disease | kidney development | β-catenin

Hepatocyte nuclear factor-1β (HNF-1β) is a homeodomain-containing transcription factor that regulates tissue-specific gene expression in the kidney, liver, pancreas, and other epithelial organs (1). In the adult kidney, HNF-1β is expressed exclusively in epithelial cells composing renal tubules and collecting ducts (2). HNF-1β is also expressed in the developing kidney, where it is essential for normal development. Ablation of *Hnf1b* in the developing mouse kidney inhibits branching morphogenesis of the ureteric bud and disrupts nephrogenesis and nephron patterning. In humans, mutations of *HNF1B* were first described in a rare autosomal dominant disease called maturity onset diabetes of the young type 5 (3). More recently, *HNF1B* mutations and deletions have been associated with a broad spectrum of kidney abnormalities including congenital anomalies of the kidney and urinary tract, autosomal dominant tubulointerstitial kidney disease (ADTKD), renal agenesis, renal hypoplasia, multicystic dysplastic kidneys, and glomerulocystic kidney disease (4). Extrarenal diseases associated with *HNF1B* mutations include hyperparathyroidism, mental retardation, autism, and gout (5). Genome-wide association studies have linked polymorphisms in *HNF1B* to prostate cancer, chromophobe renal cell carcinoma, and clear cell ovarian cancer (6).

HNF-1β and its closely related paralog, hepatocyte nuclear factor-1α (HNF-1α), have a similar structure comprising an amino-terminal (N-terminal) dimerization domain, a carboxy-terminal (C-terminal) transactivation domain, and a central POU-specific domain and POU-homeodomain responsible for DNA binding at the AT-rich consensus sequence (5′-GTTAANATTAAC-3′) (7). HNF-1β forms homodimers or heterodimers with HNF-1α to regulate gene transcription. HNF-1β can function as a transcriptional activator or repressor depending on the target gene and cellular context. In the kidney, HNF-1β regulates a network of genes involved in kidney development and tubular cell differentiation and proliferation (8). Several transgenic mouse models, including kidney-specific knockout of HNF-1β and transgenic expression of dominant-negative HNF-1β, have been generated and recapitulate phenotypes seen in humans with *HNF1B* mutations (9, 10).

Previous studies using genome-wide analysis of HNF-1β binding coupled with RNA-expression profiling have identified the genes that are directly regulated by HNF-1β in renal epithelial cells (11). These studies have revealed that HNF-1β plays a central role in cystic kidney diseases through the regulation of polycystic kidney disease (PKD) genes, such as *Pkhd1* and *Pkd2*. This approach has also identified novel roles of HNF-1β in renal cholesterol metabolism, urinary concentration, and expression of noncoding RNAs (11–13). More recently, loss of HNF-1β has been shown to induce epithelial–mesenchymal transition through dysregulation of the

## Significance

Canonical Wnt signaling plays essential roles in cell proliferation, differentiation, and survival. Binding of Wnt ligands to their receptors results in translocation of β-catenin to the nucleus, where it interacts with TCF/LEF transcription factors and activates Wnt target genes. Here, we show that the transcription factor HNF-1β competes with the binding of β-catenin/LEF complexes to DNA. We identify a composite DNA element to which HNF-1β binds and thereby inhibits β-catenin-dependent transcription. Genome-wide chromatin immunoprecipitation sequencing strikingly revealed that 50% of β-catenin-occupied sites in HNF-1β mutant cells colocalized with HNF-1β-occupied sites in wild-type cells, indicating that reciprocal binding is widespread. These studies reveal a direct transcriptional mechanism for inhibition of canonical Wnt signaling.

Author contributions: S.C.C. and P.I. designed research; M.P. contributed new reagents/analytic tools; S.C.C., Y.Z., and P.I. analyzed data; and S.C.C., Y.Z., and P.I. wrote the paper.

The authors declare no competing interest.

This article is a PNAS Direct Submission.



Data deposition: The data reported in this paper have been deposited in the Gene Expression Omnibus (GEO) database, https://www.ncbi.nlm.nih.gov/geo (accession nos. GSE130164 [RNA-seq datasets] and GSE130164 [ChIP-seq datasets]).

[1]To whom correspondence may be addressed. Email: igarashi@umn.edu.

This article contains supporting information online at www.pnas.org/lookup/suppl/doi:10.1073/pnas.1909452116/-/DCSupplemental.

First published November 11, 2019.

EMT transcription factor Twist2, which may underlie renal fibrosis in *HNF1B*-related ADTKD (8).

Pathway analysis of target genes has revealed that HNF-1β regulates intracellular signaling pathways. For example, HNF-1β constrains cyclic adenosine monophosphate (cAMP)-dependent signaling through transcriptional activation of the phosphodiesterase *Pde4c* and the polycystin-2 calcium channel that forms a complex with the calcium-sensitive adenylate cyclase AC5 (14). One of the highest-scoring pathways that emerged from the analysis of HNF-1β target genes was Wnt signaling. Wnts are secreted glycoproteins that play essential roles in embryonic development, stem cell renewal, and cell proliferation, differentiation, and survival (15). In the canonical Wnt pathway, binding of Wnt ligands to their cell-surface receptors results in β-catenin accumulation and translocation to the nucleus, where it interacts with TCF/LEF transcription factors and activates Wnt target genes (16). Deregulation of Wnt signaling occurs in diseases such as cancer and PKD (17). However, the role of HNF-1β in the regulation of Wnt signaling has not been studied previously. Here, we used next-generation RNA-sequencing (RNA-seq) and chromatin immunoprecipitation-sequencing (ChIP-seq) methods to identify Wnt-regulated gene targets in renal epithelial cells. Genome-wide analysis unexpectedly revealed a mechanism whereby HNF-1β directly represses Wnt target genes by competing with β-catenin/LEF chromatin binding.

## Results

**Ablation of HNF-1β Activates Canonical Wnt Signaling In Vitro and In Vivo.** To test whether HNF-1β plays a role in Wnt signaling, we treated HNF-1β mutant cells with the canonical Wnt ligand Wnt3a and measured the effects on β-catenin–dependent gene transcription. We previously used CRISPR-based gene editing to delete the first exon of *Hnf1b* in mIMCD3 renal epithelial cells (8). Deletion of exon 1 resulted in loss of HNF-1β protein and greatly reduced expression of its known downstream target genes, such as *Pkhd1*. To determine the effects on gene expression, we performed RNA-seq analysis on Wnt3a-treated HNF-1β mutant cells and compared the global transcriptome profiles with wild-type cells and untreated cells (Fig. 1*A*). Under basal conditions, we detected 2,733 genes that showed >2-fold increased or decreased expression in HNF-1β–deficient cells compared with wild-type mIMCD3 cells (*SI Appendix*, Fig. S1*A*). Treatment with Wnt3a altered the expression of 124 genes in wild-type mIMCD3 cells (*SI Appendix*, Table S1), whereas the number of Wnt-responsive genes was increased 8-fold in HNF-1β–deficient cells (*SI Appendix*, Table S2). Both the number of genes and the magnitude of changes in gene expression were increased in HNF-1β mutant cells. Among the upregulated genes were known targets of canonical Wnt signaling, such as *c-myc*, *Lef1*, and *Sp5*. These results suggest that HNF-1β–deficient cells are hyperresponsive to Wnt3a.

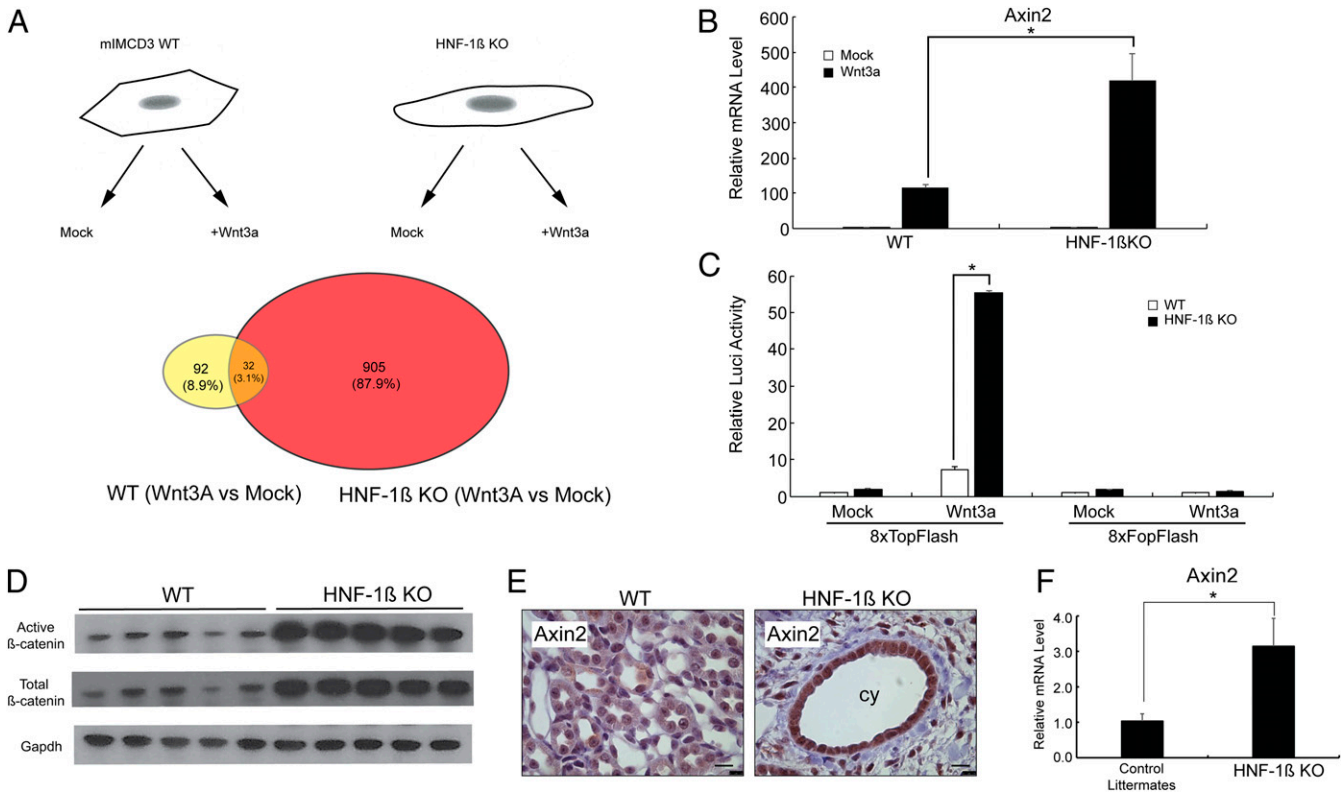


**Fig. 1.** Activation of canonical Wnt signaling in HNF-1β–deficient renal epithelial cells and HNF-1β mutant kidneys. (*A*) Schematic diagram showing RNA-seq analysis of wild-type mIMCD3 cells (WT) and HNF-1β–deficient cells (KO) following treatment with Wnt3a (100 ng/mL) or vehicle (mock). The Venn diagram shows the number of differentially expressed genes in wild-type cells (yellow) and HNF-1β–deficient cells (red). (*B*) Quantitative RT-PCR showing increased levels of *Axin2* transcripts in HNF-1β–deficient cells (KO) compared to wild-type mIMCD3 cells (WT) following Wnt3a treatment. Data shown represent the means of 3 independent cell lines. Error bars indicate SE. $^*P < 0.05$. (*C*) Luciferase activity measured in wild-type mIMCD3 cells (open bars) and HNF-1β–deficient cells (solid bars) following transfection with 8×TopFlash or 8×FopFlash reporter plasmids and treatment with Wnt3a or vehicle (mock). Data shown represent the means of the 3 independent transfections. Error bars indicate SD. $^*P < 0.05$. (*D*) Immunoblot showing increased levels of active (dephosphorylated) β-catenin and total β-catenin in protein lysates from HNF-1β mutant kidneys (KO) compared to wild-type kidneys (WT) ($n = 5$). GAPDH was used as a loading control. (*E*) Immunohistochemical staining of kidney sections from P28 control mice (*Left*) and HNF-1β mutant mice (*Right*) using an anti-Axin2 antibody ($n = 3$). (Scale bar, 10 μm.) (*F*) Quantitative RT-PCR showing increased expression of *Axin2* in P28 HNF-1β mutant kidneys compared to wild-type littermates. Data shown represent means ± SE. $^*P < 0.05$ ($n = 3$).

KEGG pathway analysis confirmed that ablation of HNF-1β resulted in the activation of known Wnt target genes as well as activation of Wnt-interacting pathways, including TGF-β signaling, axonal guidance, cytokine function, and cancer (*SI Appendix*, Fig. S1*B*). The well-established canonical Wnt gene target *Axin2* was the most up-regulated gene based on RNA-seq analysis. To confirm this finding, we performed quantitative reverse transcription–PCR (RT-PCR) on total RNA from 3 independent wild-type mIMCD3 cell lines and 3 HNF-1β–deficient cell lines. Treatment with Wnt3a increased the levels of *Axin2* mRNA transcripts 110-fold in HNF-1β–deficient cells compared to 420-fold in wild-type cells (Fig. 1*B*). To confirm that HNF-1β–deficient cells were hyperresponsive to Wnt3a, we performed luciferase reporter assays. Wild-type and HNF-1β–deficient cells were transfected with TOPFLASH plasmids containing a luciferase reporter gene under the control of a multimerized TCF/LEF-binding site. Treatment with Wnt3a produced a 7-fold increase in luciferase activity in wild-type cells, whereas Wnt3a produced a significantly greater 55-fold increase in luciferase activity in HNF-1β–deficient cells (Fig. 1*C*). The stimulation was specific since transfection with FOPFLASH plasmids containing mutated TCF/LEF-binding sites and treatment with Wnt3a did not result in increased luciferase activity.

To determine whether the ablation of HNF-1β activated the canonical Wnt pathway in vivo, we analyzed kidney-specific HNF-1β knockout mice that were generated using Cre/loxP recombination, as described previously (9). Kidney-specific HNF-1β knockout mice are viable at birth and develop rapidly progressive cystic kidney disease. Immunoblot analysis of kidney lysates from mice at postnatal day (P) 28 showed that the levels of active, dephosphorylated β-catenin and total β-catenin were increased in HNF-1β mutant kidneys compared to kidneys from wild-type littermates (Fig. 1*D*). Immunostaining showed increased accumulation of Axin2 protein in epithelial cells lining the cysts in mutant kidneys (Fig. 1*E*). Quantitative RT-PCR analysis revealed that the levels of transcripts encoded by the canonical Wnt target gene *Axin2* were increased 3-fold in HNF-1β mutant kidneys (Fig. 1*F*). In situ hybridization confirmed up-regulation of *Axin2* mRNA transcripts in the cyst epithelium and interstitium of HNF-1β mutant kidneys (*SI Appendix*, Fig. S4 *A*–*C*). Collectively, these findings demonstrate hyperactivation of canonical Wnt signaling in the absence of HNF-1β in kidney epithelial cells.

**HNF-1β and β-Catenin Show Reciprocal Binding to Chromatin.** To investigate the mechanism whereby ablation of HNF-1β activates canonical Wnt signaling, we performed ChIP-seq to quantify β-catenin occupancy in chromatin. We elected to perform ChIP-seq using an antibody against β-catenin rather than antibodies against the DNA-binding proteins TCF/LEF, since TCF/LEF bind chromatin constitutively and β-catenin occupancy more accurately reflects active β-catenin–dependent transcription. HNF-1β mutant renal epithelial cells and wild-type cells were treated with Wnt3a or vehicle for 16 h. Chromatin was isolated, immunoprecipitated with an anti-β-catenin antibody (or IgG as a negative control), and subjected to high-throughput DNA sequencing. After peak calling using a $P$ value of <0.001, we identified 203 peaks that were induced by Wnt3a in wild-type cells and 1,122 peaks that were induced in HNF-1β–deficient cells (Fig. 2*A* and *SI Appendix*, Table S3). Tag-density heatmaps centered on β-catenin peaks showed a stronger signal in HNF-1β–deficient cells induced by Wnt3a compared to wild-type cells or uninduced mutant cells (Fig. 2*A*). Aggregate plots of all β-catenin–occupied sites in the genome showed a much higher β-catenin ChIP-seq signal in HNF-1β–deficient cells treated with Wnt3a compared to wild-type or uninduced cells (Fig. 2*B*). These findings indicate that treatment with Wnt3a results in higher β-catenin occupancy in HNF-1β mutant cells compared to wild-type cells, which explains the observed activation of gene expression.

Next, we compared the genome-wide occupancy of β-catenin in HNF-1β mutant cells to the occupancy of HNF-1β in wild-type mIMCD3 cells, as previously determined by ChIP-seq using an HNF-1β–specific antibody (12, 18). Employing the same peak-calling parameters from the β-catenin ChIP-seq pipeline, we identified 28,614 HNF-1β–occupied sites in the mouse genome. Remarkably, we found that almost half of all β-catenin–occupied sites in HNF-1β mutant cells (557/1,122 peaks; 49.6%) overlapped with HNF-1β–occupied sites in wild-type cells (Fig. 2 *C* and *E* and *SI Appendix*, Table S4). Indeed, GenometriCorr analysis (19) showed that the 2 datasets were geometrically correlated and clustered at a genome-wide scale (*SI Appendix*, Fig. S2*A*). In contrast, only 3.9% of all HNF-1β–occupied sites in wild-type cells colocalized with β-catenin–occupied sites in mutant cells (Fig. 2*D*). Collectively, these findings provide evidence for genome-wide reciprocal binding of β-catenin and HNF-1β in renal epithelial cells.

We then used Analysis of Motif Enrichment (AME) to identify consensus transcription factor recognition sequences within the colocalized β-catenin– and HNF-1β–binding sites (20). Analysis of the 200-base pair (bp) segment around each peak summit revealed a significant enrichment of TCF/LEF motifs (Fig. 2*E* and *SI Appendix*, Table S5). These data confirmed that the β-catenin peaks corresponded to binding sites for TCF/LEF transcription factors. Additionally, we found a lower but significant enrichment of motifs for HNF-1β and HNF-1α (which bind an identical sequence), suggesting that the 557 colocalized peaks contained binding sites for both β-catenin/LEF and HNF-1β. The majority of the colocalized sites were located in intronic or intergenic regions, suggesting that they may function as cis regulatory elements in canonical Wnt activation (*SI Appendix*, Fig. S2*B*). Taken together, these studies uncover a function of HNF-1β in regulating the canonical Wnt pathway directly at a genomic level.

**HNF-1β Represses Canonical Wnt Target Genes.** To elucidate the functions of the colocalized β-catenin– and HNF-1β–binding sites, we compared the RNA-seq and ChIP-seq datasets and determined whether chromatin occupancy correlated with changes in Wnt3a-dependent gene expression. The heatmap in Fig. 3*A* shows the differential expression of 937 genes induced by Wnt3a in HNF-1β–deficient cells (left lanes). The right lanes show the number of β-catenin and/or HNF-1β–occupied sites located within 100 kilobases (kb) upstream or downstream of the gene body. Colocalized β-catenin– and HNF-1β–occupied sites (Fig. 3*A* rightmost lane) were associated with the most highly up-regulated genes in Wnt3a-treated HNF-1β mutant cells, whereas HNF-1β occupancy alone was not correlated (middle lane). More detailed analysis of the most up-regulated and down-regulated genes showed that colocalized β-catenin– and HNF-1β–occupied sites were located near highly up-regulated genes, including *Axin2*, *Ccdc80*, and *Rnf43* (*SI Appendix*, Fig. S3*A*). In contrast, colocalized sites were rarely located near down-regulated genes (*SI Appendix*, Fig. S3*B*), and there was no correlation between Wnt3a-dependent gene expression and HNF-1β occupancy alone. Taken together, these results indicate that HNF-1β normally represses Wnt-dependent gene expression. Ablation of HNF-1β leads to derepression of Wnt target genes, of which a subset of the most deregulated genes are associated with increased β-catenin binding to sites that colocalize with HNF-1β occupancy in wild-type cells.

To confirm these findings, we used lentivirus to reexpress wild-type HNF-1β protein in HNF-1β–deficient cells. We previously showed that ablation of HNF-1β causes renal epithelial cells to undergo epithelial–mesenchymal transition and adopt a spindle-shaped, fibroblast-like morphology. Transduction of HNF-1β mutant cells with GFP as a negative control (KO-GFP) did not affect the fibroblast-like morphology (Fig. 3*B*). In contrast, mutant cells transduced with wild-type HNF-1β adopted an epithelial morphology similar to GFP-transduced wild-type mIMCD3 cells. Immunoblot analysis confirmed that HNF-1β was reexpressed at

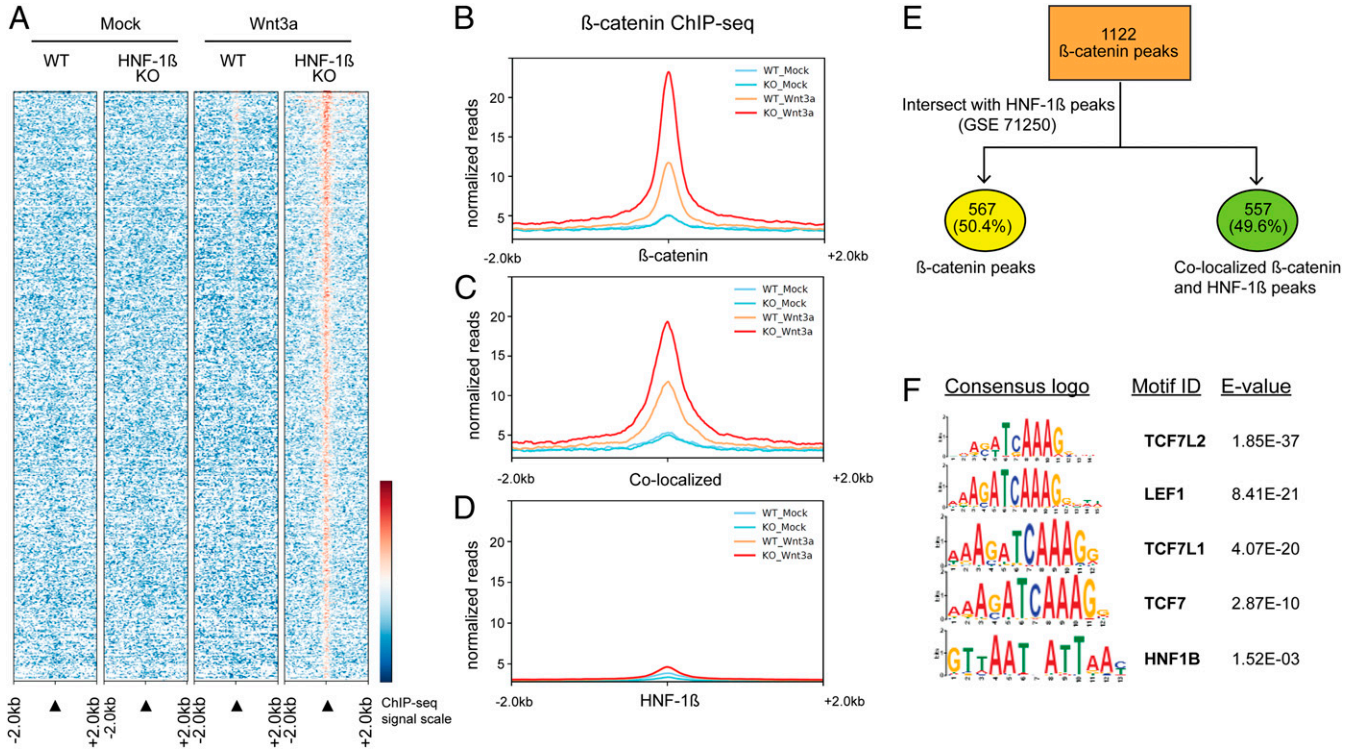


**Fig. 2.** Genome-wide colocalization of HNF-1β– and β-catenin–binding sites in renal epithelial cells. (*A*) Heatmaps showing increased β-catenin binding in chromatin from HNF-1β–deficient cells (KO) compared to wild-type mIMCD3 cells (WT) following treatment with Wnt3a (100 ng/mL). Binding is shown within a 4-kb region centered on β-catenin–binding peaks (arrowheads). Experiments were performed in duplicate. (*B–D*) Quantification of β-catenin binding at all β-catenin–binding sites (*B*), colocalized β-catenin– and HNF-1β–binding sites (*C*), and all HNF-1β–binding sites (*D*). (*E*) Schematic showing colocalized β-catenin– and HNF-1β–binding sites as a percentage of all 1,122 β-catenin–binding sites identified in this study. (*F*) Motif analysis of 557 colocalized binding sites showing enrichment of consensus recognition sequences for TCF/LEF and HNF-1β.

levels similar to those seen in wild-type cells (Fig. 3*C*). Quantitative RT-PCR showed that ablation of HNF-1β abolished the expression of its well-characterized target gene, *Pkhd1* (10). Reexpression of wild-type HNF-1β restored the expression of *Pkhd1*, demonstrating successful rescue of HNF-1β function (Fig. 3*D*). ChIP-seq identified several HNF-1β–binding sites near the *Pkhd1* locus but no individual or colocalized β-catenin–binding sites. Consequently, expression of *Pkhd1* was not affected by treatment with Wnt3a (Fig. 3*D*). In contrast, the expression of *Axin2* and *Ccdc80* was strongly up-regulated in Wnt3a-treated HNF-1β mutant cells compared to wild-type cells (Fig. 3 *E* and *F*). Reexpression of wild-type HNF-1β attenuated the robust increase in *Axin2* and *Ccdc80* transcript levels after Wnt3a treatment. Collectively, these data demonstrate a specific function of HNF-1β in repressing a subset of canonical Wnt pathway gene targets.

**Colocalized HNF-1β and β-Catenin Peaks Contain Functional Enhancers.** Inspection of β-catenin– and HNF-1β–binding sites at 2 of the most deregulated genes, *Rnf43* and *Ccdc80*, revealed strong colocalized peaks located within intron 2 and intron 6, respectively (Fig. 4 *A* and *B*). To determine whether these colocalized peaks were functional, we cloned the underlying genomic sequences into a luciferase reporter plasmid upstream of a minimal promoter. Transient transfection of the reporter plasmids into Wnt3a-treated HNF-1β–deficient cells produced higher luciferase activity than identically treated wild-type cells (Fig. 4 *C–F*). In contrast, luciferase activity produced by the empty reporter plasmid was unaffected by ablation of HNF-1β or treatment with Wnt3a. To confirm that *Rnf43* and *Ccdc80* were up-regulated in vivo, we performed antibody staining of kidney-specific HNF-1β mutant kidneys. Immunohistochemistry demonstrated increased of levels of RNF43 and CCDC80 proteins in cyst epithelial cells of HNF-1β mutant kidneys (Fig. 4 *G* and *H*). Quantitative in situ hybridization (RNAscope) confirmed that the increased protein levels reflected up-regulation of *Rnf43* and *Ccdc80* mRNA transcripts in the cyst epithelium of HNF-1β mutant kidneys (*SI Appendix*, Fig. S4 *D–I*). In addition, *Ccdc80* was up-regulated in the renal interstitium. Taken together, these results suggest that the reciprocal binding of β-catenin and HNF-1β at *cis*-regulatory elements plays a crucial role in transcriptional repression of Wnt target genes and that loss of HNF-1β leads to transcriptional derepression.

**HNF-1β and β-Catenin/LEF Compete for Binding to a Common DNA Element.** The widespread reciprocal binding of β-catenin and HNF-1β in the genome and the colocalization of binding sites raised the possibility that HNF-1β and β-catenin/LEF complexes might compete for binding to a common DNA element. We performed in-depth motif analysis of the colocalized peaks using various motif analysis programs, such as Analysis of Motif Enrichment (AME) module within MEME Suite (MEME-AME), Gibbs Sampler, ChipMuck, and Weeder (19, 21–23). All programs showed enrichment of consensus TCF/LEF motifs. Using the short-sequence motif-discovery algorithm Discriminative Regular Expression Motif Elicitation (DREME) within the MEME Suite (24), we identified several A/T-rich motifs characteristic of homeodomain binding sites. Inspection of DNA sequences containing the colocalized binding sites in *Rnf43* intron 2 and *Ccdc80* intron 6 revealed a composite site comprising a consensus half-site for HNF-1β and an overlapping TCF/LEF consensus motif (Fig. 5 *A* and *D*). To identify additional composite sites within other colocalized β-catenin– and HNF-1β–binding regions, we searched for the TCF/LEF seed motif, SWWWS (S = G or C; W = A or T),

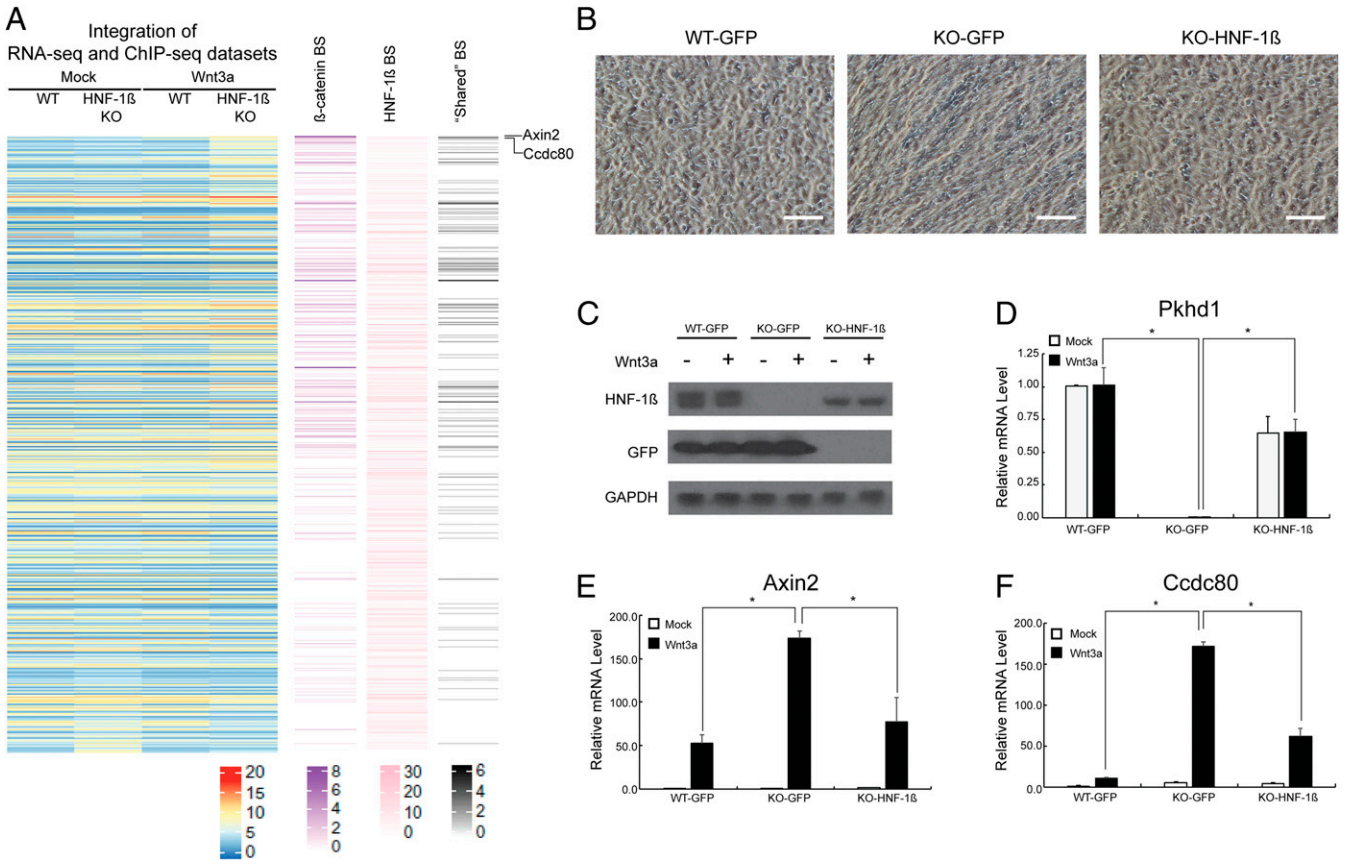


**Fig. 3.** HNF-1β directly represses canonical Wnt target genes. (*A*) Heatmaps showing the alignment of RNA-seq (*Left*) and ChIP-seq (*Right*) datasets from wild-type mIMCD3 cells (WT) and HNF-1β–deficient cells (KO) following treatment with Wnt3a or vehicle (mock). Genes are ranked based on the magnitude of changes in mRNA expression in HNF-1β–deficient cells induced with Wnt3a compared to vehicle (*Left*, lanes 1–4). The number of genomic sites occupied by β-catenin in HNF-1β–deficient cells (lane 5), sites occupied by HNF-1β in wild-type cells (lane 6), and colocalized sites (lane 7) are shown for each gene (*Right*). (*B*) Phase-contrast photomicrographs of wild-type mIMCD3 cells transduced with GFP (*Left*), HNF-1β–deficient cells transduced with GFP (*Middle*), and deficient cells transduced with HNF-1β (*Right*). (Scale bar, 100 μm.) (*C*) Immunoblot analysis of Wnt3a- or vehicle-treated cells probed with antibodies against HNF-1β, GFP, and GAPDH. (*D–F*) Quantitative RT-PCR showing expression of *Pkhd1*, *Axin2*, and *Ccdc80* in wild-type cells, HNF-1β–deficient cells, and rescued cells treated with Wnt3a (closed bars) or vehicle (open bars). Data shown represent means ± SE. $*P < 0.05$.

adjacent to an A/T-rich HNF-1β half-site, SWWWWW. Scanning the genomic sequences of the 557 colocalized peaks in both DNA strands, we identified 83 (15%) potential composite sites (*SI Appendix*, Table S6).

To confirm that TCF/LEF and HNF-1β bind to the composite elements identified in *Rnf43* and *Ccdc80*, we performed electrophoretic mobility-shift assays (EMSA). Incubation of wild-type probes with reticulocyte lysates programmed with HNF-1β or LEF1 produced retarded bands, indicating that the individual transcription factors can bind to the motif (Fig. 5 *B* and *E*). Binding was specific since mutations of the putative TCF/LEF motifs abolished binding to both HNF-1β and LEF1 (Fig. 5 *B* and *E*). Likewise, mutations of the HNF-1β half-site abolished binding to HNF-1β (*SI Appendix*, Fig. S5). Importantly, EMSA performed with wild-type probes and increasing amounts of LEF1 in the presence of a constant amount of HNF-1β revealed competition between HNF-1β and LEF1 in occupying these composite sites in vitro (Fig. 5 *C* and *F*). Mutations of the HNF-1β half-site that abolished HNF-1β binding also prevented LEF1 binding to the *Rnf43* site and reduced LEF1 binding to the *Ccdc80* site, further supporting competitive binding of HNF-1β and LEF1 to the composite element (*SI Appendix*, Fig. S5).

Previous crystal structures of HNF-1α and HNF-1β revealed that the nuclear localization signal located within the DNA-binding domain contacted DNA through a C-terminal arginine residue (25). Therefore, we mutated this arginine residue to lysine (a similar positively charged amino acid) or alanine (a neutral amino acid), as shown in Fig. 5*H*. EMSA showed that the R209K mutation decreased HNF-1β binding and the R209A mutation abolished binding to wild-type probes derived from *Rnf43* intron 2 and *Ccdc80* intron 6 (Fig. 5 *I* and *J*). In contrast, a probe derived from the *Pkhd1* promoter showed strong binding to both wild-type and mutant HNF-1β (Fig. 5 *K* and *L*) (10). Collectively, these results revealed a mode of DNA binding by HNF-1β through a composite motif at colocalized HNF-1β– and β-catenin–binding sites in the genome.

## Discussion

The transcription factor HNF-1β is essential for normal kidney development and renal tubular function. Mutations of HNF-1β disrupt ureteric branching, nephrogenesis, and nephron patterning and produce kidney cysts and tubulointerstitial fibrosis (reviewed in ref. 4). Previous studies have shown that HNF-1β directly regulates the transcription of cystic disease genes and controls pathways that are involved in kidney development (e.g., Notch signaling) and PKD (e.g., cAMP-dependent signaling) (26). Here, we identify a function of HNF-1β in the regulation of canonical (β-catenin–dependent) Wnt signaling in the kidney. Ablation of HNF-1β in renal epithelial cells using CRISPR-based gene editing results in activation of the canonical Wnt signaling pathway, as

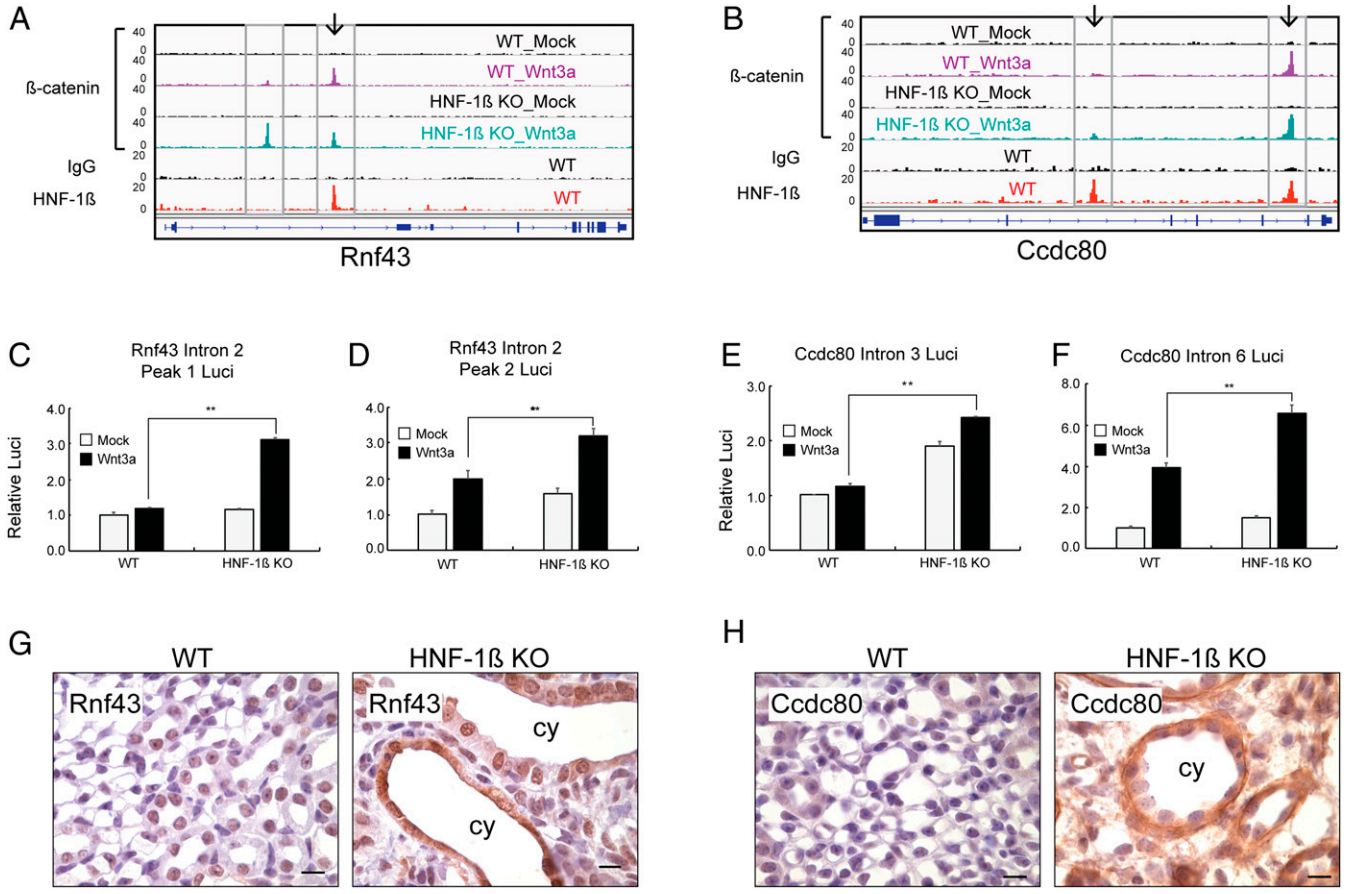


**Fig. 4.** Colocalized β-catenin– and HNF-1β–binding sites contain functional enhancers. (*A* and *B*) ChIP-seq showing the binding of β-catenin (upper lanes) to Wnt target genes, *Rnf43* and *Ccdc80*, in wild-type mIMCD3 cells (WT) and HNF-1β–deficient cells (KO) following treatment with Wnt3a or vehicle (mock). Lower lanes show binding of HNF-1β in wild-type mIMCD3 cells. ChIP-seq using IgG is shown as a negative control. Blue bars indicate exons, and arrowheads indicate the direction of transcription. Vertical arrows denote colocalized peaks. (*C*–*F*) Genomic segments containing β-catenin–binding sites were cloned into pGL4.23 luciferase reporter plasmids and transfected into wild-type (WT) and HNF-1β–deficient cells (KO). Luciferase activity was measured after treatment with Wnt3a (closed bars) or vehicle (open bars). Data shown represent means ± SD from 3 independent experiments. $^{**}P < 0.01$. (*G* and *H*) Immunohistochemical staining of kidney sections from Ksp/Cre;*Hnf1b*$^{f/f}$ mice (KO) and wild-type littermates (WT) using antibodies against RNF43 (*A*) and CCDC80 (*B*). Experiments were conducted on P28 mice in triplicate. (Scale bar, 10 μm.) cy, cyst.

evidenced by a genome-wide increase in Wnt-dependent gene expression, increased genomic occupancy by β-catenin, increased TOPFLASH luciferase reporter activity, and increased expression of the canonical Wnt target gene *Axin2*. Increased levels of Axin2 mRNA transcripts and protein associated with elevated active (dephosphorylated) β-catenin are observed in kidney-specific HNF-1β mutant mice, indicating that loss of HNF-1β also deregulates the Wnt pathway in vivo. Consistent with our findings, Haumaitre et al. (27) previously described 2 human fetuses carrying frame-shift mutations that disrupted the DNA-binding domain and C-terminal activation domain of HNF-1β. Kidney histology showed bilateral polycystic kidneys with markedly elevated β-catenin levels in the cyst epithelium. Taken together, these results indicate that HNF-1β normally constrains canonical Wnt signaling, and loss of function leads to deregulation of the pathway.

Activation of canonical Wnt signaling is likely to contribute to the HNF-1β mutant phenotype. The Wnt/β-catenin pathway stimulates cell proliferation and interstitial fibrosis, both hallmarks of HNF-1β mutant kidneys (28). In addition, multiple studies have suggested a causal link between canonical Wnt signaling and the formation and growth of kidney cysts in PKD (29). Transgenic expression of constitutively active β-catenin produces kidney cysts in mice (30). Our previous studies have shown that kidney-specific inactivation of Kif3a, a subunit of kinesin-II that is essential for cilia formation, produces kidney cysts and activation of β-catenin (31). Deletion of Apc, a negative regulator of the Wnt pathway, in renal tubules leads to the development of cysts lined by a hyperproliferative epithelium (32). The C-terminal domain of polycystin-1, a protein that is mutated in autosomal dominant PKD, interacts with β-catenin and inhibits its function (33). Mutation of polycystin-2 up-regulates β-catenin, and, conversely, knockdown of β-catenin slows cyst progression in *Pkd2* mutant mice (34). Interestingly, mutations of HNF-1β increase cell proliferation and disrupt planar cell polarity, leading to misorientation of cell division during tubule elongation (35). Activation of canonical Wnt signaling and inhibition of noncanonical signaling may underlie the disruption in planar cell polarity, leading to cystogenesis in HNF-1β mutant kidneys. Transcriptomic analysis of cystic kidneys from humans with PKD has revealed down-regulation of HNF-1β and up-regulation of Wnt pathway genes (36). Collectively, these results suggest that hyperactivation of canonical Wnt signaling plays an important role in cystic kidney disease arising from mutations of *HNF1B* and other cystic disease genes. Pharmacological inhibition of β-catenin–dependent Wnt signaling may represent a promising therapeutic approach in cystic kidney disease.

The mechanism whereby mutations of HNF-1β deregulate canonical Wnt signaling is multifactorial. Wnt/β-catenin signaling in metazoan development and tissue homeostasis has been studied

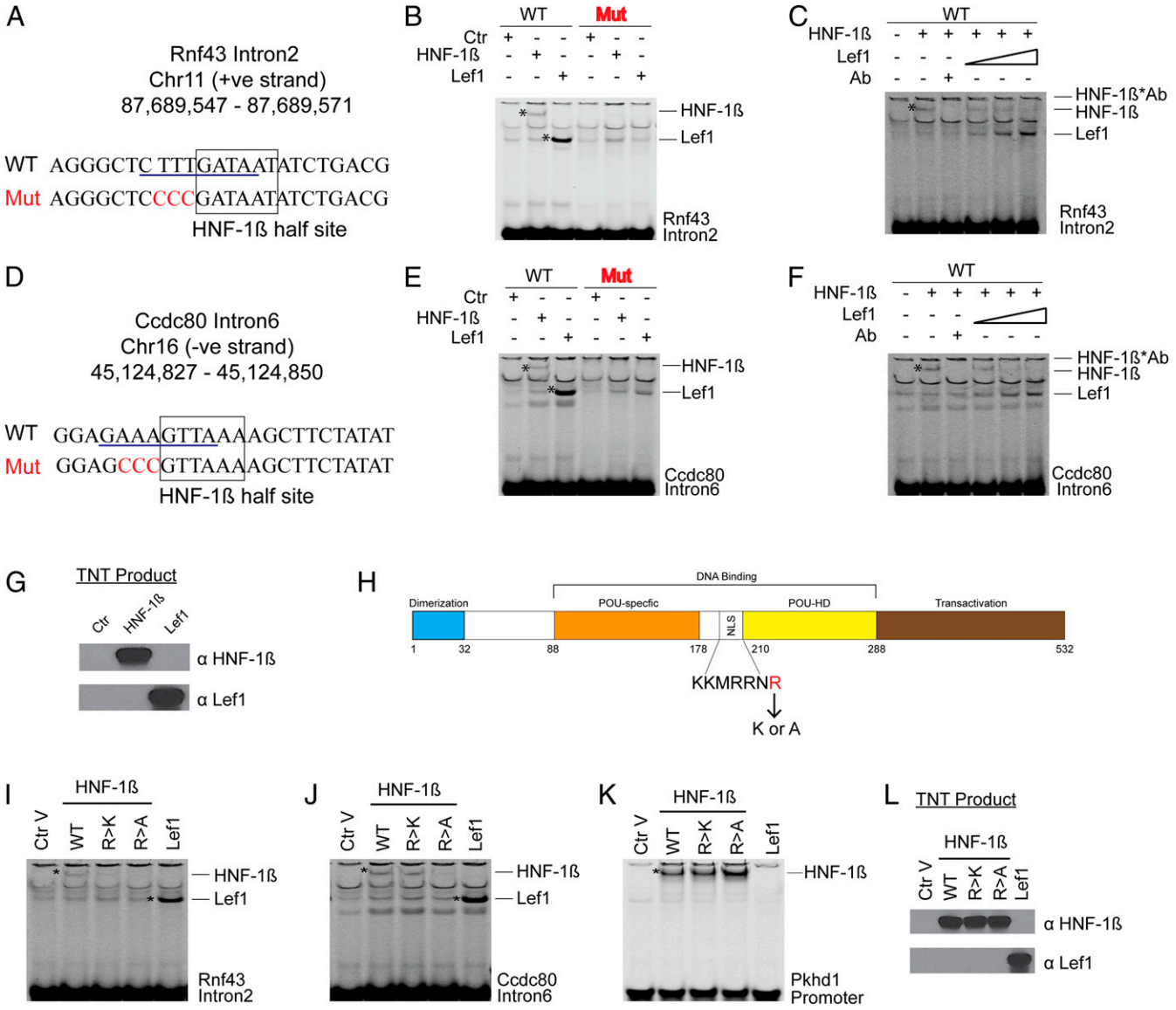


**Fig. 5.** HNF-1β competes with β-catenin for binding to a composite DNA element. (*A*) Sequence of IRD700-labeled DNA probe containing the colocalized HNF-1β– and β-catenin–binding sites within intron 2 of *Rnf43*. The black rectangle shows the consensus HNF-1β half-site, and the blue underline shows the consensus TCF/LEF motif. The mutated (Mut) probe sequence is shown in red. (*B*) EMSA binding assays were performed using wild-type (WT) or mutated (Mut) *Rnf43* probes and lysates programmed with HNF-1β, LEF1, or unprogrammed lysates (Ctr). *Retarded bands. (*C*) EMSA competition assays were performed using a constant amount of in vitro-translated HNF-1β and increasing amounts of LEF1 (lanes 4–6). Lane 3 shows EMSA supershift with the addition of HNF-1β antibody. (*D*) Sequence of IRD700-labeled DNA probe containing the colocalized HNF-1β– and β-catenin–binding sites within intron 6 of *Ccdc80*. The black rectangle shows the consensus HNF-1β half-site, and the blue underline shows the consensus TCF/LEF motif. The mutated (Mut) probe sequence is shown in red. (*E*) EMSA binding assays were performed using wild-type (WT) or mutated (Mut) *Ccdc80* probes and lysates programmed with HNF-1β, LEF1, or unprogrammed lysates (Ctr). *Retarded bands. (*F*) EMSA competition assays were performed using a constant amount of in vitro-translated HNF-1β and increasing amounts of LEF1 (lanes 4–6). Lane 3 shows EMSA supershift with the addition of HNF-1β antibody. (*G*) Immunoblot showing in vitro-translated lysates probed with antibodies against HNF-1β and LEF1. (*H*) Schematic of HNF-1β showing the location of the arginine (R209) residue that was mutated to lysine (R209K) or alanine (R209A). (*I*–*K*) EMSA binding assays using probes for *Rnf43* intron 2 (*I*), *Ccdc80* intron 6 (*J*), and *Pkhd1* promoter (*K*) and lysates programmed with wild-type HNF-1β (WT), mutant HNF-1β (R209K, R209A), or wild-type LEF1. (*L*) Immunoblot showing levels of wild-type and mutant HNF-1β and LEF1 in programmed lysates. Ctr indicates unprogrammed lysates.

for decades (15). This important signal transduction pathway is regulated at multiple steps in different cellular compartments. In the absence of Wnt signaling, cytosolic levels of β-catenin are constrained by a multiprotein complex containing Axin, APC, casein kinase 1 (CK1), and glycogen synthase kinase 3β (GSK3β). Sequential phosphorylation of the N-terminal domain of β-catenin by CK1 and GSK3β leads to β-Trcp–dependent ubiquitination and proteasomal degradation. In the nucleus, members of the TCF/LEF family of high-mobility group (HMG) DNA-binding transcription factors bind constitutively to Wnt-response elements (WRE) located near Wnt target genes. In the absence of Wnt signaling, TCF/LEF proteins are bound to Groucho-related corepressors (TLE) that induce chromatin compaction and negatively regulate the transcription of Wnt target genes. Activation of the pathway by binding of Wnt ligands to cell surface frizzled (Fz) receptors and lipoprotein receptor protein (LRP) coreceptors leads to recruitment of Axin to the plasma membrane and inhibits the phosphorylation and degradation of β-catenin. Newly synthesized β-catenin accumulates in the cytosol and translocates to the nucleus, where it binds to TCF/LEF proteins and promotes the

formation of an active enhanceosome comprising TCF/LEF, β-catenin, TLE, Pygo, BCL9, and ChiLS (37). In the present study, RNA profiling revealed that loss of HNF-1β results in up-regulation of multiple components of the Wnt pathway, including Wnt ligands (*Wnt6*, *Wnt9a*, *Wnt7b*, *Wnt11*), Fz receptors (*Fzd4*), LRP co-receptors (*Lrp4*), TCF/LEF transcription factors (*Lef1*), and pathway activators (*Lgr5*). Genome-wide ChIP-seq identified HNF-1β–binding sites located within or near some of the genes, such as *Wnt9a*, *Fzd4*, and *Lef1*. HNF-1β can function as a transcriptional repressor, an activity that may be mediated by its interaction with chromatin remodeling enzymes, such as HDAC1 (38). Therefore, one mechanism whereby HNF-1β regulates the Wnt pathway is through direct transcriptional repression of genes encoding components of the pathway, and derepression in HNF-1β mutant cells leads to Wnt hyperresponsiveness.

In addition to this conventional mechanism of transcriptional repression, we identified a second mechanism whereby HNF-1β regulates canonical Wnt signaling at enhancers through competitive binding to a composite motif consisting of a HNF-1β consensus half-site and a TCF/LEF motif. Genome-wide ChIP-seq showed that β-catenin genomic occupancy was increased 6-fold in HNF-1β mutant cells treated with Wnt3a compared to wild-type cells, consistent with activation of the canonical Wnt pathway. Unexpectedly, 50% of the genomic sites that were occupied by β-catenin in HNF-1β mutant cells colocalized with known HNF-1β–binding sites in wild-type cells. Moreover, β-catenin occupancy at the colocalized sites was increased 4-fold in HNF-1β–deficient cells compared to wild-type cells, indicating that reciprocal binding of β-catenin and HNF-1β is widespread in the mouse genome. The discovery that half of the β-catenin–occupied sites colocalize with HNF-1β–binding sites suggests a direct molecular interaction at chromatin in kidney epithelial cells. Integration of RNA-seq and ChIP-seq datasets revealed a correlation between binding and gene deregulation, suggesting that colocalization represents a mechanism whereby HNF-1β inhibits canonical Wnt activation (Fig. 3). Genomic annotation showed that the majority of the colocalized peaks are located in intronic and intergenic regions, suggesting that they represent *cis*-acting regulatory elements. Luciferase reporter assays confirmed that these newly identified enhancers are functional. (Fig. 4).

More detailed analysis of colocalized peaks located within the introns of 2 highly deregulated genes, *Rnf43* and *Ccdc80*, revealed that they contained a composite DNA element comprising a consensus TCF/LEF-binding site overlapping with an adjacent HNF-1β half-site. The sequence specificity of HNF-1β is mediated through its DNA-binding domain comprising a POU-specific domain and a POU-homeodomain. The crystal structure of human HNF-1β protein complexed with DNA demonstrated that HNF-1β binds to DNA as a dimer, and sequence specificity is conferred by a helix-turn-helix motif that projects into the major groove TCF/LEF family proteins contain HMG box are known to bind to a stretch of A or T at minor grove (39). EMSA assays demonstrated that HNF-1β and LEF1 can bind individually to the composite element located in *Rnf43* Intron 2 and *Ccdc80* Intron 6. In addition to interactions with the major groove, HNF-1β contacts the minor groove of DNA via an arginine residue located between the POU-specific domain and homeodomain (40). This residue appears to be important for binding to the hybrid element, since mutation of the arginine to alanine abolishes binding. These results suggest a DNA-binding property of HNF-1β using an adjacent TCF/LEF motif as an anchor. The interaction between HNF-1β and the composite DNA motif appears to be weaker than the binding to a full HNF-1β site (Fig. 5*K*). Importantly, competitive EMSA assays showed that HNF-1β and LEF1 compete for binding to composite motif (Fig. 5 *C* and *F*), suggesting a mechanism whereby HNF-1β inhibits Wnt enhanceosome formation by occupying the hybrid TCF/LEF motif directly.

Because of the potentially deleterious effects of Wnt pathway hyperactivity, several mechanisms have evolved to constrain the pathway. In the absence of Wnt ligands, accumulation of β-catenin is prevented by proteasomal degradation, and the interaction of TCF/LEF proteins with groucho corepressors tonically inhibits the transcription of Wnt pathway genes through chromatin compaction. Moreover, many Wnt pathway genes themselves encode negative regulators that turn off the pathway once it is activated (e.g., Axin, Naked). Here, we identify a mechanism for negative regulation of the Wnt pathway by inhibiting binding of TCF/LEF complexes at Wnt target genes. Such a mechanism would prevent expression of Wnt target genes even in the presence of activated β-catenin and could potentially inhibit functions of TCF/LEF that are independent of β-catenin (41). Further studies are needed to determine the role of the competition between TCF/LEF and HNF-1β in normal development and whether inhibiting TCF/LEF binding to the composite element identified in this study represents a more targeted approach for correcting Wnt pathway abnormalities in HNF-1β–related diseases.

## Methods

**Transgenic Mice.** Ksp/Cre mice that express Cre recombinase under the control of the *Ksp-cadherin* (*Cdh16*) promoter and *Hnf1b*$^{f/f}$ mice containing loxP sites flanking exon 1 of *Hnf1b* have been described previously (9). Ksp/Cre mice were crossed with *Hnf1b*$^{f/+}$ mice, and the bitransgenic progeny were intercrossed to generate Ksp/Cre;*Hnf1b*$^{f/f}$ mice (HNF-1β mutant mice). Cre-negative or Ksp/Cre;*Hnf1b*$^{f/+}$ littermates were used as negative controls. Mice of both sexes were used and produced equivalent results.

**Cell Culture.** mIMCD3 cells and 293T cells were obtained from the American Type Culture Collection and maintained in Dulbecco's modified Eagle's medium (DMEM) supplemented with 10% fetal bovine serum (FBS) and antibiotics (100 units/mL penicillin and 100 mg/mL streptomycin). Cells were cultured at 37 °C under 5% $CO_2$.

**Plasmids.** A lentiviral vector expressing GFP (pLV-GFP) has been described previously (42). To generate a vector expressing HNF-1β (pLV-HNF-1β), the mouse HNF-1β coding sequence (GenBank accession no. NM_001291268) was amplified with primers containing EcoRV and Sal1 restriction sites at the 5′ and 3′ ends, respectively. The PCR product was cloned in-frame into compatible restriction sites of pLV-GFP digested with 5′ EcoRV and 3′ Sal1. Genomic segments containing the colocalized β-catenin and HNF-1β peaks were amplified by PCR and cloned into a pGL4.23 plasmid upstream to the minimal promoter and luciferase reporter gene. The pcDNA3-HNF-1β expression plasmid has been described previously (11). HNF-1β mutants (R209K, R209A) were generated using QuikChange mutagenesis kits (Agilent) according to the manufacturer's instructions. A cDNA encoding Lef1 (GenBank accession no. NM_010703) was amplified by PCR and cloned downstream to the T7 promoter in the plasmid pcDNA3.1. Primers used for cloning are listed in *SI Appendix*, Table S7.

**Quantitative Real-Time PCR.** Quantitative real-time PCR was performed as described previously (8). Primers used for quantitative RT-PCR are listed in *SI Appendix*, Table S8.

**RNA-Seq.** RNA-seq and data analysis were performed as described previously (8). Briefly, wild-type mIMCD3 cells and HNF-1β–deficient cells were seeded in triplicate in 6-well plates ($5 \times 10^5$ cells/well) and cultured in DMEM containing 10% FBS. Cells were grown to 80 to 90% confluence and treated with 100 ng/mL Wnt3a (R&D Systems) or vehicle alone as a negative control. After incubation for an additional 16 h, RNA was harvested using RNeasy Mini Kits (Qiagen). TruSeq stranded mRNA libraries were created from each sample and sequenced in a 50-bp paired-end run on a HiSEq 2500 instrument using v4 chemistry. Sequencing was performed by the University of Minnesota Genomics Center. Raw and processed data have been deposited at the National Center for Biotechnology Information Gene Expression Omnibus database under accession no. GSE130164.

**ChIP-Seq.** Wild-type mIMCD3 cells and HNF-1β–deficient cells were seeded in 10-cm tissue culture dishes ($5 \times 10^6$ cells/dish) and cultured in DMEM containing 10% FBS. Cells were grown to 80 to 90% confluence and treated with 100 mg/mL Wnt3a or vehicle alone as a negative control. After incubation

for an additional 16 h, cells were fixed in 4% paraformaldehyde for 10 min at room temperature. ChIP was performed using an antibody against β-catenin (no. 8480; Cell Signaling) or isotype-specific IgG (no. 2729; Cell Signaling) as a negative control. ChIP was performed using SimpleChIP Plus Enzymatic Chromatin Kits (no. 9005; Cell Signaling) according to the manufacturer's instructions. For ChIP-seq, 100 pg of eluted DNA or input was used for library creation with ThruPLEX DNA-seq Kits (Takara Bio). Sequencing was performed by the University of Minnesota Genomics Center using an Illumina HiSEq 2500 in 1× 50-bp single-read mode.

Raw single-end ChIP-seq reads in fastq format were first assessed for base call quality, cycle uniformity, and contamination using FastQC. Raw reads were mapped to the mouse reference genome (ensemble GRCm38) via Burrows-Wheeler Aligner (43). Binding peaks were called with Model-Based Analysis for ChIP-Seq version 2.0 (MASC2) (44) using default parameters. Duplicate samples were merged into a single file, and deepTools (45) was used for data visualization. Motif exploration tools, AME (20), Gibbs Sampler (21), ChipMunk (22), and Weeder (23), were used to identify enriched motifs and scan for enrichment of known motifs. Each program was run at least twice, and common outputs were collected as enriched motifs. ChIPseek (46) was used for functional annotation of ChIP-seq peaks. R package GenometriCorr (version 1.1.17) (19) was used to test for significance of clustering between HNF-1β– and β-catenin–binding sites. Raw and processed data have been deposited at the National Center for Biotechnology Information Gene Expression Omnibus under accession no. GSE130164.

**Lentiviral Transduction.** Packaging of a lentiviral system in 293T cells for transduction of mIMCD3 cells has been described previously (47). mIMCD3 cells were infected with lentivirus and selected by hygromycin (200 μg/mL) for 10 d. Surviving cells were pooled for subsequent experiments.

**Antibody Staining.** Antibody staining was performed as described previously (8) using paraformaldehyde-fixed, paraffin-embedded tissues. For CCDC80 staining, tissues were fixed, embedded in optimal cutting-temperature compound, frozen, and sectioned. Antigen retrieval was performed by incubation in 1× Reveal Decloaker (RV100M; Biocare Medica) at 100 °C for 30 min. Slides were treated with 3% hydrogen peroxide, blocked in 100% Rodent Block M (RBM961; Biocare Medical), and incubated with primary antibodies in 10% Rodent Block overnight at 4 °C. The following primary antibodies were used: Axin2 (1:10,000 [no. 32197; Abcam]), Rnf43 (1:1,000 [no. HPA008079; Sigma]), and Ccdc80 (1:500 [no. HPA002266; Sigma]). Slides were incubated in secondary Rabbit-on-Rodent HRP-Polymer (RMR622; Biocare Medical), treated with 3-3′ diaminobenzidine (DAB) (926603-buffer A, 926503-buffer B; Biolegend), and counterstained with hematoxylin. Images were captured with a DFC7000 T camera mounted on a Leica DM5500 B upright microscope.

**Luciferase Assays.** mIMCD3 cells and HNF-1β–deficient cells were transfected with 4 μg of luciferase reporter plasmid and 1 μg of control SV40-Renilla reporter plasmid using 10 μL of Lipofectamine 3000. Transfected cells were seeded in 12-well plates ($5 \times 10^5$ cells/well) and cultured in DMEM containing 10% FBS. After 36 h, cells with treated with Wnt3a (50 ng/mL) or vehicle alone and incubated for an additional 16 h. Cells were harvested in 200 μL of lysis buffer, and 40 μL was used for measurement of luciferase activity with Dual Luciferase Assay kits (Promega). Raw data were normalized by dividing firefly luciferase activity by Renilla luciferase activity.

**EMSA.** EMSA was performed using a modification of a previously described protocol (42). The forward- and reverse-strand EMSA DNA probes were labeled with 5′ IRD700 and purified by high-performance liquid chromatography (IDT). Probe sequences are shown in *SI Appendix*, Table S9. The DNA duplexes (10 pmol/μL) were annealed and diluted to a final working concentration of 2.5 nM. EMSA was performed using Odyssey EMSA Kits (LI-COR 829-07910) according to the manufacturer's instructions. In vitro-translated proteins were prepared using a TNT reticulocyte translation system (no. L1170; Promega). cDNAs were cloned into a T7-driven expression vector for in vitro transcription and translation of the encoded proteins. Binding reactions were incubated at room temperature for 30 min. EMSA mixtures were then resolved using tris(hydroxymethyl)aminomethane·glycine polyacrylamide gels. EMSA signals were detected with an Odyssey scanner (LI-COR) at 700 nm. Images were analyzed by Image Studio software (LI-COR). Unprogrammed lysates were used as negative controls.

**Immunoblot Analysis.** Immunoblot analysis was performed as described previously (47). Antibodies used for the studies are listed in *SI Appendix*, Table S10.

**In Situ Hybridization.** In situ hybridization (RNAscope) was performed as described previously (8) using commercial probes (Advanced Cell Diagnostics) against *Axin2* (catalog no. 400331; GenBank accession no. NM_015732.4), *Rnf43* (catalog no. 400371; GenBank accession no. NM_172448.3), and *Ccdc80* (catalog no. 492391; GenBank accession no. NM_026439.2). Hybridization signals were detected after kit amplification and incubation with DAB. Images were captured using a Leica DM5500 B upright microscope with DFC7000T camera. The average number of brown dots per cell was quantitated using the Image J processing package (https://fiji.sc) according to the technical guidelines provided by Advanced Cell Diagnostics.

**Statistical Analysis.** Student's 2-tailed unpaired *t* test was used for pairwise comparisons. $P < 0.05$ was considered significant.

**Study Approval.** All experiments involving animals were performed under the auspices of the Institutional Animal Care and Use Committee at the University of Minnesota.

**ACKNOWLEDGMENTS.** We thank Svetlana Avdulov for technical assistance, Mark Murphy, and Micah Gearhart for advice on ChIP and EMSA, Colleen Forster for histology support and consultation (Bionet, Clinical and Translational Science Institute, University of Minnesota), and Sachin Hajarnis for performing the preliminary studies on this project. Illumina sequencing services were performed by the University of Minnesota Genomics Center, and the Minnesota Supercomputing Institute provided bioinformatic, software support, and data storage. This work was supported by NIH Grant R37DK042921 (to P.I.).

1. P. Igarashi, X. Shao, B. T. McNally, T. Hiesberger, Roles of HNF-1beta in kidney development and congenital cystic diseases. *Kidney Int.* **68**, 1944–1947 (2005).
2. M. O. Ott, J. Rey-Campos, S. Cereghini, M. Yaniv, vHNF1 is expressed in epithelial cells of distinct embryonic origin during development and precedes HNF1 expression. *Mech. Dev.* **36**, 47–58 (1991).
3. Y. Horikawa *et al.*, Mutation in hepatocyte nuclear factor-1 beta gene (TCF2) associated with MODY. *Nat. Genet.* **17**, 384–385 (1997).
4. S. Ferre, P. Igarashi, New insights into the role of HNF-1beta in kidney (patho)physiology. *Pediatr. Nephrol.* **34**, 1325–1335 (2019).
5. J. C. Verhave, A. P. Bech, J. F. Wetzels, T. Nijenhuis, Hepatocyte nuclear factor 1β-associated kidney disease: More than renal cysts and diabetes. *J. Am. Soc. Nephrol.* **27**, 345–353 (2016).
6. D. D. Yu, S. W. Guo, Y. Y. Jing, Y. L. Dong, L. X. Wei, A review on hepatocyte nuclear factor-1beta and tumor. *Cell Biosci.* **5**, 58 (2015).
7. D. B. Mendel, L. P. Hansen, M. K. Graves, P. B. Conley, G. R. Crabtree, HNF-1 alpha and HNF-1 beta (vHNF-1) share dimerization and homeo domains, but not activation domains, and form heterodimers in vitro. *Genes Dev.* **5**, 1042–1056 (1991).
8. S. C. Chan *et al.*, Mechanism of fibrosis in *HNF1B*-related autosomal dominant tubulointerstitial kidney disease. *J. Am. Soc. Nephrol.* **29**, 2493–2509 (2018).
9. L. Gresh *et al.*, A transcriptional network in polycystic kidney disease. *EMBO J.* **23**, 1657–1668 (2004).
10. T. Hiesberger *et al.*, Mutation of hepatocyte nuclear factor-1beta inhibits Pkhd1 gene expression and produces renal cysts in mice. *J. Clin. Invest.* **113**, 814–825 (2004).
11. S. S. Hajarnis *et al.*, Transcription factor hepatocyte nuclear factor-1β (HNF-1β) regulates microRNA-200 expression through a long noncoding RNA. *J. Biol. Chem.* **290**, 24793–24805 (2015).
12. K. Aboudehen *et al.*, Transcription factor hepatocyte nuclear factor-1β regulates renal cholesterol metabolism. *J. Am. Soc. Nephrol.* **27**, 2408–2421 (2016).
13. K. Aboudehen *et al.*, Hepatocyte nuclear factor-1$\beta$ regulates urinary concentration and response to hypertonicity. *J. Am. Soc. Nephrol.* **28**, 2887–2900 (2017).
14. Y. H. Choi *et al.*, Polycystin-2 and phosphodiesterase 4C are components of a ciliary A-kinase anchoring protein complex that is disrupted in cystic kidney diseases. *Proc. Natl. Acad. Sci. U.S.A.* **108**, 10679–10684 (2011).
15. R. Nusse, H. Clevers, Wnt/β-catenin signaling, disease, and emerging therapeutic modalities. *Cell* **169**, 985–999 (2017).
16. B. T. MacDonald, K. Tamai, X. He, Wnt/beta-catenin signaling: Components, mechanisms, and diseases. *Dev. Cell* **17**, 9–26 (2009).
17. J. Yu, D. M. Virshup, Updating the Wnt pathways. *Biosci. Rep.* **34**, e00142 (2014).
18. K. Aboudehen, P. Igarashi, Hnf-1β ChIP-Seq. Gene Expression Omnibus. https://www.ncbi.nlm.nih.gov/geo/query/acc.cgi?acc=GSE71250. Deposited 23 July 2015.
19. A. Favorov *et al.*, Exploring massive, genome scale datasets with the GenometriCorr package. *PLOS Comput. Biol.* **8**, e1002529 (2012).
20. F. A. Buske, M. Bodén, D. C. Bauer, T. L. Bailey, Assigning roles to DNA regulatory motifs using comparative genomics. *Bioinformatics* **26**, 860–866 (2010).
21. W. Thompson, S. Conlan, L. A. McCue, C. E. Lawrence, Using the Gibbs motif sampler for phylogenetic footprinting. *Methods Mol. Biol.* **395**, 403–424 (2007).
22. V. G. Levitsky *et al.*, Application of experimentally verified transcription factor binding sites models for computational analysis of ChIP-Seq data. *BMC Genomics* **15**, 80 (2014).
23. G. Pavesi, G. Mauri, G. Pesole, An algorithm for finding signals of unknown length in DNA sequences. *Bioinformatics* **17** (suppl. 1), S207–S214 (2001).

24. T. L. Bailey, DREME: Motif discovery in transcription factor ChIP-seq data. *Bioinformatics* **27**, 1653–1659 (2011).
25. Y. I. Chi *et al*., Diabetes mutations delineate an atypical POU domain in HNF-1alpha. *Mol. Cell* **10**, 1129–1137 (2002).
26. C. Heliot *et al*., HNF1B controls proximal-intermediate nephron segment identity in vertebrates by regulating Notch signalling components and Irx1/2. *Development* **140**, 873–885 (2013).
27. C. Haumaitre *et al*., Severe pancreas hypoplasia and multicystic renal dysplasia in two human fetuses carrying novel HNF1beta/MODY5 mutations. *Hum. Mol. Genet.* **15**, 2363–2375 (2006).
28. Y. Wang, C. J. Zhou, Y. Liu, Wnt signaling in kidney development and disease. *Prog. Mol. Biol. Transl. Sci.* **153**, 181–207 (2018).
29. P. Goggolidou, Wnt and planar cell polarity signaling in cystic renal disease. *Organogenesis* **10**, 86–95 (2014).
30. S. Saadi-Kheddouci *et al*., Early development of polycystic kidney disease in transgenic mice expressing an activated mutant of the beta-catenin gene. *Oncogene* **20**, 5972–5981 (2001).
31. F. Lin *et al*., Kidney-specific inactivation of the KIF3A subunit of kinesin-II inhibits renal ciliogenesis and produces polycystic kidney disease. *Proc. Natl. Acad. Sci. U.S.A.* **100**, 5286–5291 (2003).
32. C. N. Qian *et al*., Cystic renal neoplasia following conditional inactivation of apc in mouse renal tubular epithelium. *J. Biol. Chem.* **280**, 3938–3945 (2005).
33. M. Lal *et al*., Polycystin-1 C-terminal tail associates with beta-catenin and inhibits canonical Wnt signaling. *Hum. Mol. Genet.* **17**, 3105–3117 (2008).
34. A. Li *et al*., Canonical Wnt inhibitors ameliorate cystogenesis in a mouse ortholog of human ADPKD. *JCI Insight* **3**, 95874 (2018).
35. E. Fischer *et al*., Defective planar cell polarity in polycystic kidney disease. *Nat. Genet.* **38**, 21–23 (2006).
36. X. Song *et al*., Systems biology of autosomal dominant polycystic kidney disease (ADPKD): Computational identification of gene expression pathways and integrated regulatory networks. *Hum. Mol. Genet.* **18**, 2328–2343 (2009).
37. M. Gammons, M. Bienz, Multiprotein complexes governing Wnt signal transduction. *Curr. Opin. Cell Biol.* **51**, 42–49 (2018).
38. E. Barbacci *et al*., HNF1beta/TCF2 mutations impair transactivation potential through altered co-regulator recruitment. *Hum. Mol. Genet.* **13**, 3139–3149 (2004).
39. M. van de Wetering, H. Clevers, Sequence-specific interaction of the HMG box proteins TCF-1 and SRY occurs within the minor groove of a Watson-Crick double helix. *EMBO J.* **11**, 3039–3044 (1992).
40. P. Lu, G. B. Rha, Y. I. Chi, Structural basis of disease-causing mutations in hepatocyte nuclear factor 1beta. *Biochemistry* **46**, 12071–12080 (2007).
41. L. Grumolato *et al*., β-Catenin-independent activation of TCF1/LEF1 in human hematopoietic tumor cells through interaction with ATF2 transcription factors. *PLoS Genet.* **9**, e1003603 (2013).
42. S. C. Chan *et al*., Targeting chromatin binding regulation of constitutively active AR variants to overcome prostate cancer resistance to endocrine-based therapies. *Nucleic Acids Res.* **43**, 5880–5897 (2015).
43. H. Li, R. Durbin, Fast and accurate short read alignment with Burrows-Wheeler transform. *Bioinformatics* **25**, 1754–1760 (2009).
44. J. Feng, T. Liu, B. Qin, Y. Zhang, X. S. Liu, Identifying ChIP-seq enrichment using MACS. *Nat. Protoc.* **7**, 1728–1740 (2012).
45. F. Ramirez, F. Dundar, S. Diehl, B. A. Gruning, T. Manke, deepTools: A flexible platform for exploring deep-sequencing data. *Nucleic Acids Res.* **42**, W187–W191 (2014).
46. T. W. Chen *et al*., ChIPseek, a web-based analysis tool for ChIP data. *BMC Genomics* **15**, 539 (2014).
47. S. C. Chan, Y. Li, S. M. Dehm, Androgen receptor splice variants activate androgen receptor target genes and support aberrant prostate cancer cell growth independent of canonical androgen receptor nuclear localization signal. *J. Biol. Chem.* **287**, 19736–19749 (2012).